J Comput Aided Mol Des (2013) 27:221–234
DOI 10.1007/s10822-013-9644-8

Protein and ligand preparation: parameters, protocols, and influence on virtual screening enrichments

G. Madhavi Sastry · Matvey Adzhigirey · Tyler Day · Ramakrishna Annabhimoju · Woody Sherman

Received: 14 December 2012 / Accepted: 3 April 2013 / Published online: 12 April 2013

Abstract Structure-based virtual screening plays an important role in drug discovery and complements other screening approaches. In general, protein crystal structures are prepared prior to docking in order to add hydrogen atoms, optimize hydrogen bonds, remove atomic clashes, and perform other operations that are not part of the x-ray crystal structure refinement process. In addition, ligands must be prepared to create 3-dimensional geometries, assign proper bond orders, and generate accessible tautomer and ionization states prior to virtual screening. While the prerequisite for proper system preparation is generally accepted in the field, an extensive study of the preparation steps and their effect on virtual screening enrichments has not been performed. In this work, we systematically explore each of the steps involved in preparing a system for virtual screening. We first explore a large number of parameters using the Glide validation set of 36 crystal structures and 1,000 decoys. We then apply a subset of protocols to the DUD database. We show that database enrichment is improved with proper preparation and that neglecting certain steps of the preparation process produces a systematic degradation in enrichments, which can be large for some targets. We provide examples illustrating the structural changes introduced by the preparation that impact database enrichment. While the work presented here was performed with the Protein Preparation Wizard and Glide, the insights and guidance are expected to be generalizable to structure-based virtual screening with other docking methods.

Keywords Virtual screening · Protein preparation · Protein preparation wizard · PrepWizard · Docking · Enrichment · Ligand preparation · Epik

Introduction

Structure-based virtual screening plays an important role in the drug discovery process and there are many examples of successes from both academia and industry [1–7]. In addition, there have been a number of publications comparing the performance of different programs in a pursuit to find the best docking methods. Some studies have looked at the ability to accurately position ligands [8–10] while others have been focused on retrieving active compounds from virtual database screens [11–17] or inverse screening for targets [18–21]. In most cases, these studies used a single protocol for the preparation of the proteins, ligands, and waters, although some of the papers have explored individual aspects of the preparation process [22–25]. The advantage of using a single preparation protocol for docking assessment studies is that it simplifies the analysis by removing many of the variables associated with virtual screening. However, there are several disadvantages, such as the fact that docking to the wrong state of a protein or not including the correct ligand tautomers does provide useful information about the quality of the docking programs; in fact, better programs could be disproportionately more negatively affected when inaccuracies in the input

Electronic supplementary material The online version of this article (doi:10.1007/s10822-013-9644-8) contains supplementary material, which is available to authorized users.

G. Madhavi Sastry · R. Annabhimoju
Schrödinger, Sanali Infopark, 8-2-120/113, Banjara Hills, Hyderabad 500034, Andhra Pradesh, India

M. Adzhigirey · T. Day · W. Sherman (✉)
Schrödinger, 120 West 45th Street, New York, NY 10036, USA
e-mail: woody.sherman@schrodinger.com

structures exist. In addition, docking with a single preparation protocol does not provide insights into best practices for virtual screening.

Many of the early docking studies focused on accurately reproducing the crystallographic poses of ligands ("native docking") [26–30]. This presents a best-case scenario in which the protein is ideally formed to accommodate the ligand of interest. As docking accuracy improved over time, there was a transition to focus more on virtual screening enrichment [31–33] and binding energy estimation [34–37], both of which are still primarily done in the context of a single rigid receptor structure. However, in recent years there has been significant progress in the treatment of receptor flexibility in docking [38–44]. Still, accurate cross docking is a challenge for the field, especially when induced-fit effects involve more than a few side-chain movements and/or subtle backbone relaxation. Furthermore, treating receptor flexibility during docking adds significant computational costs due to the increased degrees of freedom, thereby making it generally inaccessible for large-scale virtual screening campaigns.

In virtual screening, the primary objective is to score large libraries of compounds (often in the millions) and preferentially rank active compounds ahead of inactive compounds. The degree to which active compounds can be scored better than inactive compounds is referred to as "enrichment". The objective of virtual screening is typically to retrieve the maximum number of active and diverse ligands as early as possible in the rank-ordered set of results. Due to the large computational resources required for fully sampling protein and ligand atoms simultaneously, the standard approach in structure-based virtual screening is to treat the receptor rigidly, which has proven to be successful in many cases, as noted by the references provided in the preceding paragraphs. However, there is evidence that including some amount of receptor flexibility in virtual screening, either through explicit sampling or docking to an ensemble of receptor conformations, can improve results [45–51].

In this work, we focus on the preparation steps involved in docking to a single receptor structure with the aim of determining the influence of each step and the best overall protocol for virtual screening. The preparation process can be as simple as adding hydrogens, bond orders, and formal charges to the starting protein and ligand molecules. However, more involved preparation protocols include sampling degrees of freedom that are ambiguous in crystal structures of standard resolution, such as 180° flips of the terminal rotatable side-chain groups of shape-symmetric residues (Asn, Gln, and His), tautomer/ionization state assignment for both the ligand and the protein, and the treatment of residues with missing density. In addition, the placement of rotatable hydrogen atoms on Cys, Ser, Thr, and Tyr side chains can be optimized. The preparation process can also include relaxation of the receptor structure and options for the treatment of crystallographic water molecules. First, we describe the various parameters that will be explored and perform an extensive survey of the

Table 1 List of targets, PDB codes, and the number of active ligands for the exploratory set

Target	PDB code	# Actives	Target	PDB code	# Actives
Acetylcholinesterase	1e66	28	Human estrogen receptor	1err	10
Acetylcholinesterase	1eve	28	Human estrogen receptor	3ert	10
Aldose reductase	1ah3	36	Lymphocyte-specific tyrosine kinase (Lck)	1qpe	20
Aldose reductase	1ef3	36	Matrix metalloproteinase-2	1hov	20
Aldose reductase	2acq	36	Matrix metalloproteinase-3	1g49	20
Cyclin dependent kinase 2	1aq1	20	Neuraminidase	1a4q	20
Cyclin dependent kinase 2	1dm2	20	Neuraminidase	1bji	20
Cyclooxygenase-2	1cvu	33	Neuraminidase	1mwe	20
Cyclooxygenase-2	1cx2	33	p38 MAP kinase[b]	1a9u	29
E. coli thymidylate synthase	1ddu	20	p38 MAP kinase[b]	1bl7	29
E. coli thymidylate synthase	1syn	20	p38 MAP kinase[c]	1kv2	20
EGFR tyrosine kinase	1ml7	20	Squalene synthase	1ezf	20
Factor Xa	1fjs	20	Thermolysin	1tmn	10
HIV-1 protease	1hpx	15	Thrombin	1dwc	16
HIV-1 protease	1hsh	15	Thrombin	1ett	16
HIV-1 reverse transcriptase	1ep4	33	Thrombin	1mu6	16
HIV-1 reverse transcriptase[a]	1rt1	33	Thymidine kinase	1kim	7
HIV-1 reverse transcriptase	1vrt	33	Thymidylate synthase	2bbq	20

[a] Allosteric binding site

[b] ATP binding site (DFG-in)

[c] Allosteric binding site (DFG-out)

Table 2 Ligand and protein preparation settings explored in this study

Stage of preparation	Value	Description
Ligand states (ionizer/ tautomerizer or Epik)	None	Ligand states generated from LigPrep with default ionizer and tautomerizer
	Epik pH = 7 ± 2	Epik state penalties based on Hammett and Taft equations
	Epik with metal binding states	Epik state penalties with pH range expanded to 7 ± 4 and elimination of state penalty during docking if penalized atom is interacting directly with a metal
H-bond optimization (ProtAssign)	None	Retain Asn, Gln, and His rotamers from the PDB structure. Treat all His in neutral form with protonation on Nε. Asp and Glu in negative ionized form. Add hydroxyl and thiol hydrogens in default trans position
	Standard	Complete sampling of all states for H-bond clusters with up to 100 combinations. Monte Carlo sampling for clusters with more than 100 possible states
	Exhaustive	Complete sampling of all states for H-bond clusters with up to 10,000 combinations. Monte Carlo sampling for clusters with more than 10,000 possible states
Protein minimization (Impref)	H-only	Two-step relaxation of only hydrogen atoms with all other atoms fixed. In the first step, all torsional potentials to hydrogen atoms are removed
	Heavy atom RMSD = 0.15	H-only optimization followed by all-atom minimization with termination based on convergence or reaching a heavy atom RMSD of 0.15 Å
	Heavy atom RMSD = 0.30	Same as above with RMSD of 0.30 Å
	Heavy atom RMSD = 0.50	Same as above with RMSD of 0.50 Å

parameters on the Glide validation set, which includes 36 crystal structures covering 20 unique targets and the 1,000-compound Glide decoy set. We then present virtual screening enrichments on the DUD database for a subset of four protocols that range from a minimally prepared system to a fully prepared system. Finally, we show examples where particular steps in the preparation process are crucial in order to obtain good virtual screening results.

Methods

Ligand datasets

Two independent sets of ligands were used for this study. First, in order to exhaustively study all combinations of the preparation settings explored in this work, we used the Glide docking validation set with 36 crystal structures spanning 20 targets and 7–36 active compounds per target (referred to as "exploratory set") [52]. Multiple crystal structures were used for some targets to assess the enrichment variability. The Glide docking decoy set of 1,000 compounds was used, which is comprised of molecules with properties that resemble those of the active compounds [53]. We used the "400 mw" decoys set (average molecular weight of 400 Daltons) for all targets except thymidine kinase (PDB code 1kim), for which the "360 mw" decoy set was used because of the smaller active compounds. The list of targets, PDB codes, and number of active ligands for the exploratory set is provided in Table 1.

A second set of ligands for this study (referred to as "DUD test set") was obtained from the Directory of Useful Decoys based on work by Huang et al. [54]. This set includes 40 targets with ligands that have been carefully selected to ensure diversity within the active compounds and a per-target curated set of decoy molecules that have similar properties to the active compounds for that target. The DUD set was used to assess a subset of the settings examined with the exploratory set.

Ligand preparation

Three-dimensional (3D) coordinates were generated for all ligands with LigPrep [55]. Ionization/tautomeric states were generated with either a pair of fast rule-based programs (called the ionizer and tautomerizer) or with Epik [56, 57], which is based on the more accurate Hammett and Taft methodologies. In addition to calculating reasonable ligand states, Epik also estimates a penalty to quantify the energetic cost it takes to generate each state in solution. The Epik state penalty is computed in units of kcal/mol, thereby making it directly compatible with the GlideScore used for docking and allowing us to explore the impact of adding the Epik state penalty to the GlideScore. The sum of the GlideScore and the Epik state penalty is referred to as the DockingScore in Glide. The DockingScore is used for the final ranking and enrichment calculations. Epik also has a mode to treat metal binding states, which involves increasing the pH range for the state generation step and then reducing the penalty in the docking stage for states

Table 3 Enrichment statistics for virtual screening calculations run on the exploratory set with different preparation protocols

Enrichment metric	Min.	Max.	Mean	Median
HTVS				
BEDROC($\alpha = 160.9$)	0.28	0.38	0.34	0.34
BEDROC($\alpha = 20$)	0.37	0.43	0.41	0.41
EF(1 %)	17.8	23.2	21.1	21.5
SP				
BEDROC($\alpha = 160.9$)	0.30	0.42	0.37	0.38
BEDROC($\alpha = 20$)	0.42	0.53	0.49	0.50
EF(1 %)	20.6	27.8	24.8	25.4

Each value refers to an average enrichment from the 36 targets. Statistics are computed separately for the Glide HTVS and SP

where a negative charge is satisfied when binding to a metal ion.

Protein datasets

The proteins for this study were obtained from Protein Data Bank [58, 59]. The exploratory set from our Glide validation work contains 36 structures and the full list is shown in Table 1. The DUD test set is based on the work of Huang et al. [54] and contains 40 targets (see target list on the DUD website: http://dud.docking.org/r2).

Protein preparation

The Protein Preparation Wizard (PrepWizard) in Maestro [60] was used to prepare the proteins in this study. Table 2 lists all of the settings explored in this work along with a brief description. Below we describe each of the settings.

H-bond optimization (ProtAssign)

The hydrogen bonding (H-bond) network was optimized by sampling 180° flips of the terminal chi angle for Asn, Gln, and His, which significantly changes the spatial H-bonding capabilities of the side chains, but does not appreciably change the fit to the electron density. Neutral and protonated states of His, Asp, and Glu were also sampled along with the two His tautomers (proton on either the Nδ or Nε nitrogen). In addition, hydrogens on hydroxyls and thiols were sampled to optimize the H-bond network. The ProtAssign algorithm can be run in a "standard" mode that typically takes a few seconds or an "exhaustive" mode where many more states are considered, which can run for minutes or hours depending on the complexity of the H-bond networks. The standard mode performs full sampling of all states for H-bond clusters with up to 100 combinations and Monte Carlo sampling for clusters with more than 100 possible states. The exhaustive mode performs sampling of all states for H-bond clusters with up to 10,000 combinations and Monte Carlo sampling for clusters with more than 10,000 possible states.

Protein minimization (Impref)

In the recommended protein preparation protocol, after H-bond optimization, the entire structure is allowed to relax using the Impref module of Impact [61] and the OPLS_2005 force field [62–64]. The options explored for protein minimization included hydrogen only or all-atom with a termination criterion based on the root-mean-square deviation (RMSD) of the heavy atoms relative to their initial location.

Waters

The treatment of explicit water molecules can influence docking accuracy and enrichment results, as previously demonstrated by others [23, 65–69]. However, the determination of which waters to retain is difficult, primarily because the free energy of a water molecule is not directly related to the crystallographic occupancy [70]. While it was not our intention to exhaustively explore all possible treatments of water molecules, we explored one specific consideration: whether or not to keep water molecules in the structure for the H-bond optimization and protein minimization stages. It is possible, for example, that without explicit water molecules the protein could collapse in unphysical ways or that hydrogen bonding networks required for ligand binding would be disrupted. In the case where water molecules were retained through the H-bond optimization and minimization stages, all water molecules were removed prior to docking. A more extensive study of

Table 4 Enrichment results for targets in the exploratory set using three H-bond optimization settings with ProtAssign

Enrichment metric	None	Standard sampling	Exhaustive sampling
HTVS			
BEDROC($\alpha = 160.9$)	0.33	0.34	0.34
BEDROC($\alpha = 20$)	0.42	0.43	0.43
EF(1 %)	21.2	22.4	23.2
SP			
BEDROC($\alpha = 160.9$)	0.34	0.39	0.38
BEDROC($\alpha = 20$)	0.48	0.50	0.50
EF(1 %)	22.6	26.6	26.2

Results are for no Impref minimization with all water molecules removed and the ligands prepared with Epik using metal binding states. Larger values are better

the role of waters in docking and how to incorporate water energetics will be the focus of a future publication.

Docking

All docking calculations were performed with Glide v5.7 [71]. Calculations were run in either the HTVS mode (High-Throughput Virtual Screening) using default settings (1–2 s for a typical drug-like compound) or the SP mode (Standard Precision), which performs more extensive sampling (10–20 s per compound). Docking grids were generated with the default settings in Glide using the co-crystalized ligand to define the center of the grid box.

Enrichment calculations

For enrichment calculations, we saved the top pose for each ligand (based on Emodel) and ranked all ligands by the DockingScore. The DockingScore consists of the GlideScore plus any additional penalties associated with the Epik tautomer/ionization state assignment for the ligands. We report the enrichment factor (EF) for the top 1 % of the database as well as the Boltzmann-enhanced discrimination of the receiver operating characteristic (BEDROC) [72]. We use $\alpha = 160.9$ and $\alpha = 20$ for the BEDROC calculations, the former corresponding to 80 % of the maximum contribution to the BEDROC score being accounted for in the top 1 % of the database screen and the latter corresponding to 80 % of the score being accounted for in the top 8 % of the screen. In all cases, earlier parts of the hit list count more heavily in the BEDROC score based on a Boltzmann weighting. Although BEDROC has highly desirable characteristics, such as a smooth functional form that is not highly sensitive to small changes in the ranking of compounds around a specific cutoff value and being more sensitive to the very early part of the ROC curve, we continue to use the more common EF(1 %) metric because it can be compared directly to results from other papers and the numerical results are in general more intuitive to understand. We do not present results using the popular area under the receiver-operating characteristic curve (AUC) because that metric is not good for assessing early enrichment. For example, an ROC curve with a value of 0.5 is generally interpreted as random; however, if 50 % of the actives are retrieved in the earliest part of the screen and the other 50 % of the actives are missed completely that will result in an AUC of 0.5, yet the results are highly predictive in the early part of the ROC curve. Such results may indicate that there are multiple binding modes or significant induced-fit effects that allow only a subset of the ligands to dock well. However, the EF(1 %), BEDROC($\alpha = 160.9$), and BEDROC($\alpha = 20$) metrics would correctly produce enrichment results significantly better than random.

Results

In this work, we perform an extensive study of steps involved in the protein and ligand preparation process by varying the settings in the Protein Preparation Wizard within Maestro and evaluating the effects on virtual screening enrichments. In total, 2,592 virtual screening calculations (36 targets, 3 LigPrep settings, 3 H-bond assignment settings, 4 minimization settings, and 2 docking modes) were performed on an exploratory dataset

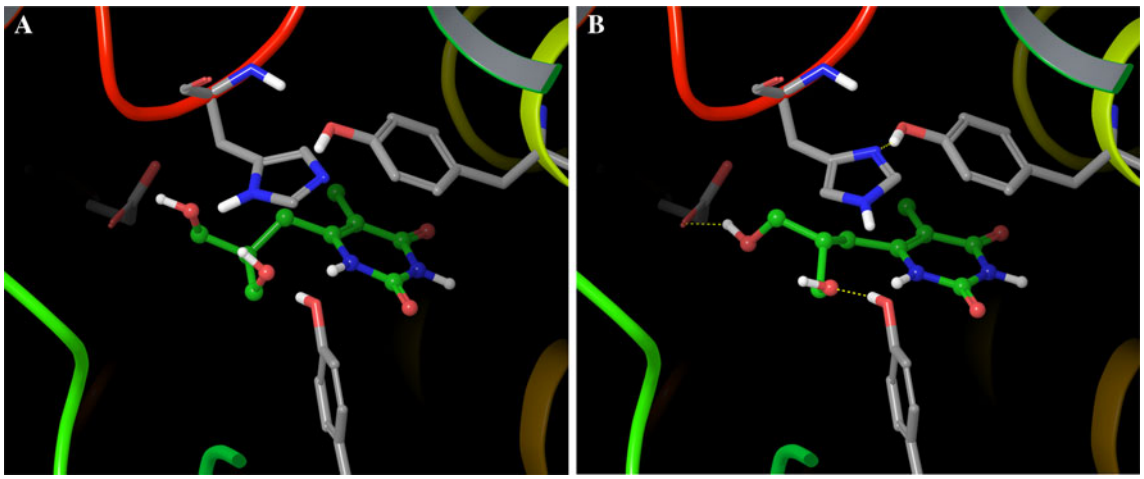

Fig. 1 Thymidine kinase (1kim) example of ProtAssign H-bond optimization. **A** His58 before applying ProtAssign sampling makes no hydrogen bonds to either the ligand or the protein. **B** After ProtAssign sampling His58 changes tautomer and flips 180° in the terminal chi angle, resulting in an intramolecular H-Bond with Tyr172 (*yellow dotted line*). In addition, ProtAssign also generates hydrogen bonds from the ligand to Tyr101 and Glu83

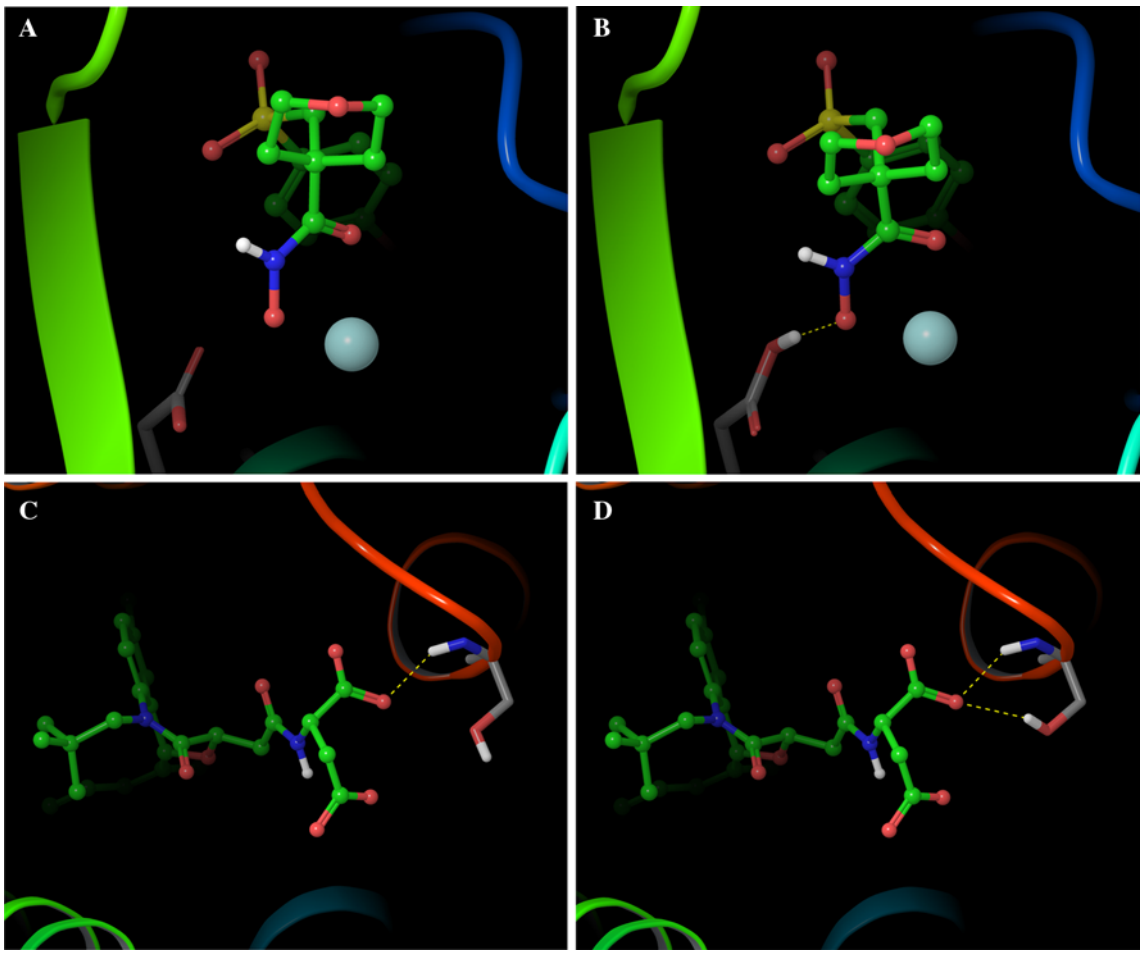

Fig. 2 Examples where ProtAssign improves the scoring of an active ligand. **A** MMP3 (1g49) without ProtAssign no hydrogen bond is formed with Asp702. **B** With ProtAssign the carboxylate group of Asp702 is protonated, resulting in an H-bond with the hydroxamic acid group of the ligand (*yellow dotted line*). In addition, the orientations of the hydroxyl group of Tyr720 and the protonation state of His724 differ between the two cases. The active ligand shown is ranked 22 (not in the top 1 %) when ProtAssign is not used and improves to 10 (in the top 1 %) when ProtAssign sampling is performed. Similarly, the EF(1 %) values improve from 15.2 to 30.3 with ProtAssign. **C** Squalene synthase (1ezf) without ProtAssign forms only one H-bond from the carboxylate to the receptor. **D** ProtAssign samples the Ser53 hydroxyl to form an H-bond with the native ligand

consisting of 1,000 decoys and 7–36 actives per target (the Glide validation set). We then apply a subset of the preparation protocols to forty targets from DUD. The enrichment statistics for the exploratory set aggregated over all of the virtual screening calculations with Glide HTVS and SP (36 virtual screening calculations for each of the 36 targets in the exploratory set for each docking mode) are shown in Table 3.

Table 3 shows that the enrichment results vary, on average, between the virtual screening calculations with different preparation settings and that there is a significant difference between the best and worst protocol. However, the averages across 36 targets mask the true variability that can be observed for a single target, since a given stage in the preparation process may not matter for one protein but might have a large effect for another protein. In the following sections, we first analyze the variability in enrichment for each individual step of the preparation process keeping the other steps fixed. We then provide a meta-analysis where the combined preparation process is separated into minimal, intermediate, and full preparation of the protein plus a final setting that combines full protein preparation plus full ligand preparation.

H-bond optimization (ProtAssign)

The H-bond optimization step (called ProtAssign) creates the best network of hydrogen bonds by placing/rotating hydrogens and functional groups that do not impact the electron density (Asn, Gln, and His). The optimized state was then subjected to force field minimization of only hydrogen atoms while keeping all other atoms fixed.

Table 5 Enrichment results for targets in the exploratory set using four minimization settings with Impref

Enrichment metric	Heavy atom RMSD cutoff			
	0.0 Å	0.15 Å	0.30 Å	0.50 Å
HTVS				
BEDROC($\alpha = 160.9$)	0.33	0.36	0.37	0.36
BEDROC($\alpha = 20$)	0.43	0.42	0.43	0.41
EF(1 %)	22.4	22.0	22.8	21.1
SP				
BEDROC($\alpha = 160.9$)	0.39	0.40	0.42	0.41
BEDROC($\alpha = 20$)	0.50	0.51	0.53	0.52
EF(1 %)	26.6	26.0	27.0	27.8

Results are for default ProtAssign sampling with all water molecules removed and the ligands prepared with Epik using metal binding states

Table 4 shows the results for three ProtAssign settings (none, standard, and exhaustive; see Table 2 and Methods for definitions). There is a significant improvement when ProtAssign sampling is performed. A majority of the targets (20 of 36) show improvement in the EF(1 %) values when performing ProtAssign sampling, while 5 targets show degradation and 11 show no change in enrichment. Table S1 in the Supporting Information provides all of the enrichment values for each target and for each setting.

ProtAssign sampling ensures that an optimized H-bond network is generated for interactions with the co-crystalized ligand, which is likely to be a good configuration for other active ligands as well. However, binding of different ligands can induce changes in the protein that are not accounted for in the rigid receptor docking work performed here. To account for such effects one would need to consider a structural ensemble or sample receptor flexibility explicitly in docking; neither of these directions was explored in this work. Interestingly, the exhaustive sampling does not provide improvement over standard sampling, suggesting that in most cases the standard sampling is sufficient to generate a good H-bond network for docking.

As an example of the effect of H-bond optimization, a large improvement in enrichment is observed for thymidine kinase (1kim) after running ProtAssign, where the EF(1 %) enrichment increases from 57.8 to 86.6 (50 % improvement). In this case, ProtAssign flips the terminal torsion of His58 by 180° and exchanges the proton from the Nδ position to the Nε position, thereby forming an H-bond with Tyr172 (see Fig. 1). This H-bond is known to be important for binding to ribose and pyrimidine derivatives [73]. Interestingly, many of the good scoring active ligands dock far from His58, so it is unlikely that the change in His58 has a direct impact in the DockingScore of the active compounds. However, we notice that the scores of the docked compounds in general improve when ProtAssign sampling is used. For example, the average DockingScore of the actives improves from −9.3 to −9.6 kcal/mol. However, the average DockingScore of the decoys in the top 1 % database increases almost as much (from −9.1 to −9.3 kcal/mol). Figure 1 shows His58 in the initial state and the state after ProtAssign in thymidine kinase. The active shown in Fig. 1 improves from rank 46 to 11.

Aldose reductase (2acq) and HIV protease (1hpx) are other cases where large improvements are seen with H-bond optimization. For aldose reductase the EF(1 %) increases from no signal to a value of 16.8 upon protassign sampling. The primary structural change is seen in His110, which exhibits a change in tautomer and a 180° flip relative to the crystal structure that leads to a hydrogen bond with the co-crystal ligand. This hydrogen bond is not possible with the crystal structure histidine state, either with the proton on the Nδ or Nε position. In addition, Asn160 and Gln183 undergo side chain amide flips. In the case of HIV protease, the EF(1 %) improves from 47.2 to 60.6 as a result of one of the catalytic Asp residues becoming protonated to share a hydrogen between the two Asp residues upon H-bond optimization.

Figure 2A shows an example where H-bond optimization in MMP3 (PDB code 1g49) correctly determines the H-bond network, thereby resulting in an increased enrichment, from 15.2 to 20.2 for EF(1 %). With H-bond optimization the carboxylate group of Glu702 is protonated, resulting in an H-bond with the ligand. In addition, the orientation of the hydroxyl group of Tyr720 and the protonation state of His724 make improved interactions with the ligand after H-bond optimization. The active ligand shown in Fig. 2A is ranked 22 when H-bond optimization is not performed, whereas it improves to 10 (in the top 1 %) after H-bond optimization, with a DockingScore improvement from −10.7 to −12.3 kcal/mol. Figure 2B shows an example in squalene synthase (PDB code 1EZF; also called farnesyl-diphosphate farnesyltransferase) where H-bond optimization improves the orientation of the Ser53 hydroxyl to form an H-bond with the native ligand.

Five targets show decreases between 3.1 and 10.8 in the EF(1 %) values. In the case of HIV reverse transcriptase (1ep4) and acetylcholinesterase (1eve), the decreases are relatively small. However, another acetylcholinesterase structure (1e66) shows the maximum decrease in enrichments upon ProtAssign sampling. With ProtAssign, His440 becomes protonated along with a rotation in the hydroxyl group of Ser200. This results in the loss of an H-bond between Ser200 and His440 residues. In addition, Tyr130 exhibits a change in the hydroxyl torsion. These changes result in a reduction in the Coulombic contribution to the DockingScore for many of the actives. For example, the

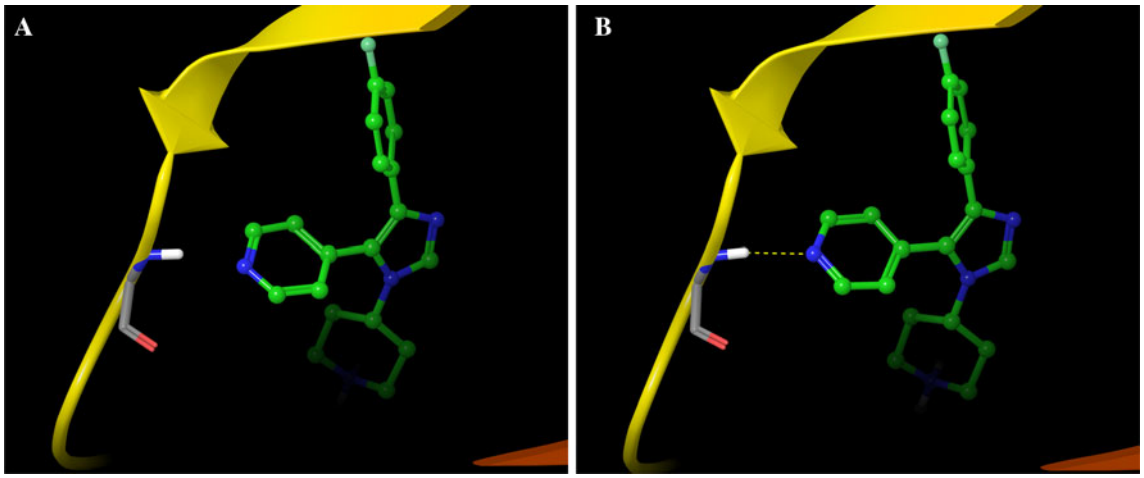

Fig. 3 Effect of Impref RMSD on an active ligand of P38 MAP kinase (1a9u). **A** Keeping the heavy atoms fixed during minimization. **B** Minimization with RMSD of 0.3 Å results in a better hydrogen bond interaction with the backbone of Met109 in the hinge (*yellow dotted line*)

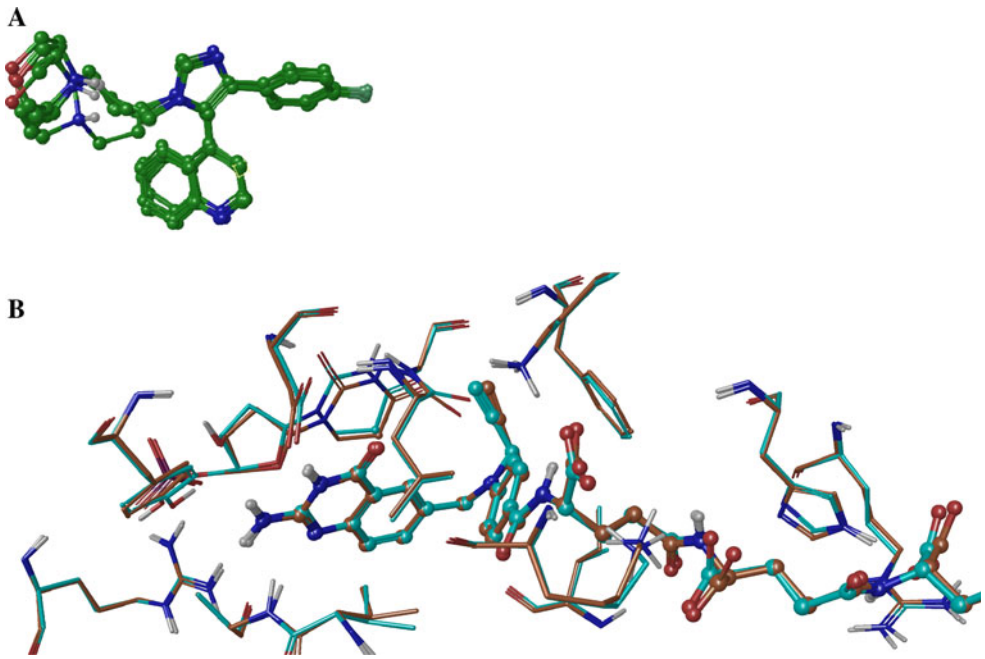

Fig. 4 Structural changes with different Impref minimization RMSD cutoffs. **A** P38 MAP kinase (1a9u; DFG-in) co-crystalized ligand minimized with Impref RMSD cutoff of 0.15, 0.3, and 0.5 Å. **B** Active site of thymidylate synthase (2bbq) showing minimal structural difference when minimized by restraining all heavy atoms and minimized with 0.3 Å RMSD cutoff. The *blue* and *brown colored carbons* distinguish between the two structures

average Coulomb energy of all the docked actives is −5.9 kcal/mol with ProtAssign and −8.7 kcal/mol without ProtAssign. Looking at the Coulombic contribution for the docked decoys in the top 1 % of the database, the average Coulomb energy when ProtAssign is used is −13.1 and −14.4 kcal/mol when no ProtAssign is used. It should be noted that the actives and high-ranking decoys of acetylcholinesterase contain charged groups. In the case of 1eve, His440 does not get protonated by ProtAssign and the H-bond is retained with Ser200, resulting in higher enrichment. Cases like this indicate that manual inspection of the protein before docking is important to correct any errors or inconsistencies introduced into the structure during automatic preparation.

Protein minimization (Impref)

Next we explored the effect of protein minimization using the Impact [61] refinement module (Impref). Impref involves a 2-step relaxation where first the rotatable hydrogen atoms are allowed to minimize with the torsional potential removed, which is followed by a full minimization of all atoms that is terminated either when the system is fully converged or when it reaches a user-specified RMSD cutoff for the heavy atoms. Here, we explored no minimization of the heavy atoms (hydrogens only) or an RMSD cutoff value of 0.15, 0.30, or 0.5 Å for the heavy atoms. Table 5 shows the average enrichment results with three Impref settings applied after standard sampling in

Table 6 Enrichment results for targets in the exploratory set using three ligand preparation settings

Enrichment metric	Ionizer/ tautomerizer	Epik	Epik + metal binding states
HTVS			
BEDROC($\alpha = 160.9$)	0.34	0.37	0.38
BEDROC($\alpha = 20$)	0.39	0.42	0.43
EF(1 %)	22.0	22.1	22.8
SP			
BEDROC($\alpha = 160.9$)	0.37	0.41	0.42
BEDROC($\alpha = 20$)	0.48	0.51	0.53
EF(1 %)	24.4	26.6	27.0

Results are for standard ProtAssign sampling and Impref minimization using a 0.3 Å RMSD with all water molecules removed during the preparation

ProtAssign. As seen, the minimization protocol improves the average enrichments, with the best value for both HTVS and SP being obtained with an RMSD cutoff of 0.30 Å. In total, 16 systems get better, 9 systems get worse, and 11 systems remain unchanged in terms of EF(1 %) in the SP docking mode after running minimization. In terms of BEDROC($\alpha = 20$) enrichments, 23 targets show improvement while the remaining 13 targets show a degradation.

The target showing the most significant improvement in enrichment upon Impref minimization is P38 MAP kinase (1a9u), which improves the EF(1 %) from 13.9 to 24.4. Interestingly, the structural changes were subtle, with most of the differences being in loops around the active site. Figure 3 shows the formation of an added hydrogen bond to the hinge when Impref minimization is done with an active compound whose rank improves from 18 (DockingScore −7.7 kcal/mol) to 3 (DockingScore −8.8 kcal/mol) with heavy atom relaxation using an Impref RMSD of 0.3 Å. Figure 4A shows an example of the structural changes in the ligand with different RMSD cutoffs for P38 MAP kinase. The hinge H-bond interaction in kinases is very important for molecular recognition and binding affinity. The small movements of atoms from the minimization improve this interaction, highlighting that even subtle changes in protein structure can have a large effect on virtual screening enrichments.

As with the previous results for H-bond optimization, we also find a few cases where enrichments get worse with minimization, such as thymidylate synthase (2bbq), which degrades from EF(1 %) of 40.4–30.3. The exact reasons for the degradation are not entirely clear, since the structural changes are minimal. Figure 4B shows the superposition of the binding site residues before and after the minimization. In most of the cases where enrichment degrades, the exact cause is difficult to pinpoint.

Ligand preparation (LigPrep and Epik)

Next, we explored the effect of ligand preparation, where tautomers and ionization states were generated with either the ionizer/tautomerizer utilities (simple pattern matching for functional groups) or Epik (based on the Hammett and Taft methodologies, which account for substituent effects). In addition to generating states, Epik also assigns an energetic penalty for each ligand state, which can be added to the GlideScore to produce the final DockingScore. We also explored a mode in Epik to account for metal binding states, which generates higher-energy states that have the possibility to recuperate the energetic cost upon binding to a metal ion. Table 6 shows the enrichment results for each of the three ligand preparation settings on the Glide exploratory set. Epik shows a consistent improvement over the ionizer/tautomerizer (7.7 % BEDROC improvement for HTVS and 6.3 % for SP) and Epik with metal binding states shows a further improvement (10.2 % BEDROC improvement for HTVS and 10.4 % for SP). A total of 23 systems get better and 13 systems get worse after running Epik with metal binding states based on the BEDROC($\alpha = 20$) metric.

Looking at the three targets with metal binding sites (thermolysin, MMP-2, and MMP-3), the average improvement in BEDROC($\alpha = 20$) is 77.4 % for SP and 71.9 % for HTVS when using the metal binding states mode of Epik over using simply Epik without special metal binding states, emphasizing the importance of generating the right ligand states for binding to metals (see Table 7). In addition, including metal binding states does not significantly degrade the enrichment for targets without metals in the binding site, validating that inclusion of metal-specific binding states and the associated penalty term is handled adequately with Glide. The metal binding mode has the most significant effect on MMP2 and MMP3. The metal binding groups for MMP2 and MMP3 are mainly based on hydroxamic acid derivatives, which are neutral at pH 7 ± 2 and require the special metal binding state treatment in Epik to generate the negative forms, hence the significant improvement in enrichments when using the metal binding mode in Epik for MMP2 and MMP3. The metal binding mode of Epik has minimal effect on thermolysin, since the active compounds contain either carboxylate or phosphate metal binding groups, which are already deprotonated at pH 7.0.

The largest improvements in enrichment when including Epik calculations come from squalene synthase (1ezf), thymidylate synthase (1syn), and thymidine kinase (1kim), which show an improvement in EF(1 %) of 25.3, 20.2, and 14.4, respectively. In many cases, decoy molecules get very good docking scores when prepared with the ionizer/tautomerizer because unreasonable states are generated

Table 7 Enrichment results for targets in the exploratory set with metal binding sites

Target	PDB code	Enrichment metric	HTVS		SP	
			Epik	Epik + metal binding states	Epik	Epik + metal binding states
Matrix metalloproteinase-2	1hov	BEDROC($\alpha = 160.9$)	0.006	0.20	0.11	0.33
		BEDROC($\alpha = 20$)	0.13	0.30	0.19	0.40
		EF(1 %)	0.0	15.2	5.0	20.2
Matrix metalloproteinase-3	1g49	BEDROC($\alpha = 160.9$)	0.38	0.52	0.35	0.39
		BEDROC($\alpha = 20$)	0.30	0.52	0.29	0.63
		EF(1 %)	20.2	30.3	20.2	20.2
Thermolysin	1tmn	BEDROC($\alpha = 160.9$)	0.41	0.42	0.65	0.65
		BEDROC($\alpha = 20$)	0.60	0.67	0.65	0.68
		EF(1 %)	30.3	30.3	60.6	60.6

Results are for standard ProtAssign sampling and Impref minimization using a 0.3 Å RMSD cutoff with all water molecules removed during the preparation

without an associated energetic penalty. For example, squalene synthase has several decoys that produce multiply charged ligands states with the ionizer that score better than the singly charged ligand states. There are four decoys in the top 1 % database with formal charges ranging between −3 and −5. They receive good GlideScore values due to the strong electrostatic interactions that are not compensated by the associated penalty required to generate the state. Figure 5 shows some of the top scoring squalene synthase decoys along with the docking ranks and Epik state penalties. As can be seen, these compounds all have high Epik state penalties. Epik would not have generated most of them even with the pH 7.0 ± 4.0 setting. For those cases that would have been generated, their DockingScore would not have placed them in the top 1 % of the database screen.

As an example, the ionizer generates state B4 in Fig. 5, which has a formal charge of +5 and an Epik state penalty of 26.5 kcal/mol. Not considering the energetic penalty of generating this state, the ligand ranks #3 in the database screen as a result of some very favorable electrostatic interactions that get reflected in the GlideScore. However, penalizing this state by adding the Epik penalty to the GlideScore to produce the DockingScore prevents it from competing with any of the active compounds and would place it near the end of the screening hit list. Indeed, Epik does not even generate this state with the settings used in this work. Similarly B1, B2, and B3 in Fig. 5 score well with the GlideScore, but have Epik state penalties of 4.0, 17.6, and 21.0 kcal/mol, respectively. Again, adding the Epik state penalty to the GlideScore to obtain the DockingScore results in these decoy compounds scoring significantly worse in the screening hit list.

While using the ionizer/tautomerizer generally yields more states than Epik, some of which are unreasonable (see preceding paragraphs), it also misses some important states due to the simple pattern-based rules. Some examples of ionization/tautomer states for active ligands generated by Epik and not with the ionizer/tautomerizer are shown in Fig. 6. These compounds typically contain multiple nitrogen atoms in a single ring or conjugated ring system where a single pattern-based system would have difficulties unless the exact pattern was encoded. On the other hand, the methodology in Epik accounts for more complex systems and substitution effects, thereby finding many more of the relevant ionization and tautomer states. For the active compounds in Fig. 6, they are all retrieved in the top 1 % of the database screen when Epik is used for preparation whereas none of them are in the top 1 % with ionizer/tautomerizer preparation.

Analysis of DUD screening results

To simplify the analysis of all of the settings explored here, we compressed the 36 possible combinations of settings into 4 general levels of preparation: Minimal, Intermediate, Full, and Full + Ligand. Minimal preparation involves only minimizing hydrogen atoms. Intermediate adds ProtAssign H-bond optimization. Full preparation adds Impref minimization of the protein with RMSD of 0.3 Å after H-bond optimization. Finally, Full + Ligand adds Epik ligand preparation with metal binding states to the Full protocol. The enrichment results for these 4 protocols run on the Glide validation set and DUD exploratory sets with the HTVS mode of Glide are shown in Table 8.

We see that more complete protein preparation consistently results in higher enrichments. For example, the average EF(1 %) enrichment obtained for the Glide validation set using HTVS Glide docking with the Minimal preparation is 17.8 whereas the best results of 22.8 are obtained with Full + Ligand preparation (28 % improvement over Minimal preparation). Similar improvements

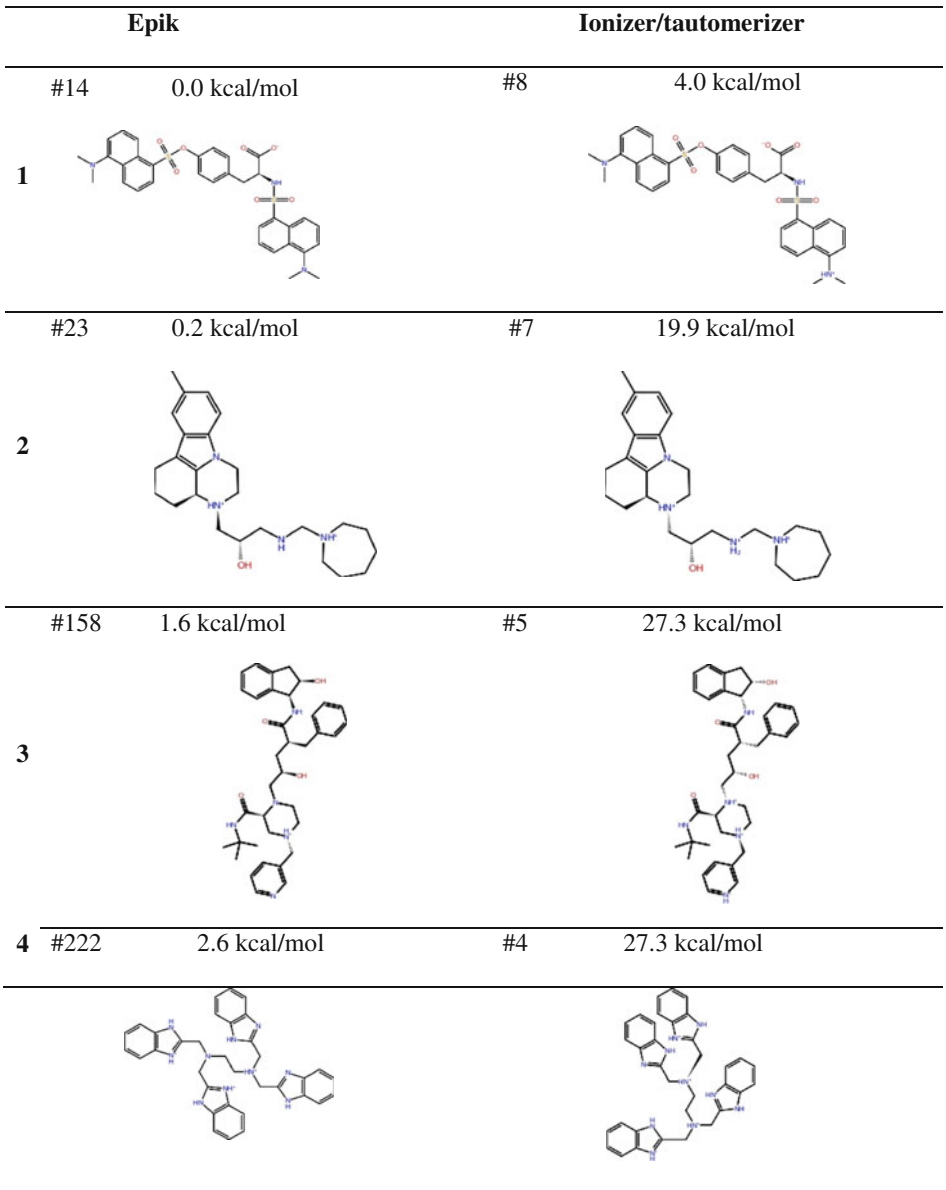

Fig. 5 Decoys of squalene synthase (1ezf) generated by Epik (*left*) and the ionizer/tautomerizer (*right*). The ranks (*above left*) in the docking screen and Epik state penalty (above) are shown. As discussed in the text, unreasonable states generated by the ionizer/tautomerizer lead to poor enrichments due to artificially good scoring of decoys arising from favorable interactions with the receptor that are not properly compensated by the appropriate ionization/tautomer penalty

(21 %) are observed on the DUD test set for the HTVS docking mode. In addition, Full + Ligand produces the best average results for the Glide exploratory set using Glide SP as well (31 % improvement of Full + Ligand over Minimal on the Glide exploratory set). In addition, the observed improvements when applying more complete preparation are statistically significant, as seen in Table 9, based on p value analysis as proposed by Nicholls for evaluating virtual screening results [74]. The advantage of Full + Ligand over the Minimal and Intermediate preparation protocols is significant at the 0.05 level for both the Glide exploratory set and DUD test set. The advantage of Full + Ligand over Full preparation is less significant, suggesting that including Epik ligand preparation does not improve results as much as the protein preparation steps. Nonetheless, the Full + Ligand preparation is, on average, better than the Full preparation without including Epik states for the ligands for the Glide exploratory set and DUD test set.

The role of water

Up to this point, all systems were prepared with water molecules removed prior to any preparation steps. However, it is interesting to consider the implications of preparing the targets with binding site waters present and then removing them before docking. Doing this, we found very little change in average enrichments if water molecules were retained or eliminated prior to the protein preparation process. For example, with the Full + Ligand preparation,

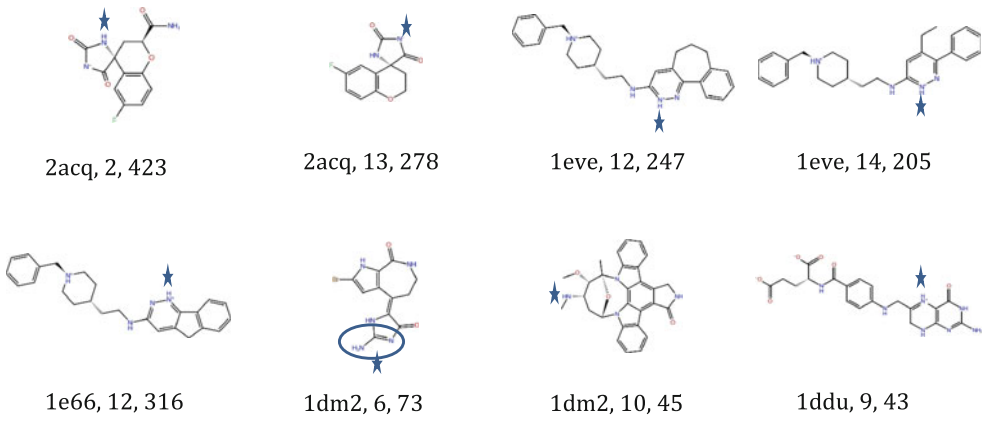

Fig. 6 States for active ligands generated by Epik and not with the ionizer/tautomerizer. Each active is annotated by target, best rank from docking the Epik generated ligand states, and best rank from the ionizer/tautomerizer generated states. The *star* denotes the location where Epik produces a good state for docking that is missed by the ionizer/tautomerizer. All ranks are from Glide SP

Table 8 Average EF(1 %) enrichment values for the Glide exploratory set and DUD test set using four preparation protocols

Database	Preparation			
	Minimal	Intermediate	Full	Full + ligand
Glide	17.8	19.7	22.1	22.8
DUD	12.0	12.2	14.1	14.6

Minimal involves minimizing only the hydrogen coordinates. Intermediate preparation adds H-bond network optimization prior to hydrogen minimization. Full preparation adds protein minimization (RMSD = 0.3 Å) after H-bond optimization. Full + Ligand preparation adds Epik ligand preparation to the Full protein preparation

Table 9 Significance level of the EF(1 %) enrichment differences between the preparation protocols shown in Table 8

	Min	Inter	Full	Full + ligand
Glide				
Min	1	0.952	0.999	1.000
Inter	0.047	1	0.974	0.980
Full	0.001	0.025	1	0.732
Full + ligand	0.000	0.020	0.268	1
DUD				
Min	1	0.624	0.996	0.986
Inter	0.376	1	0.972	0.96
Full	0.004	0.028	1	0.682
Full + ligand	0.014	0.04	0.318	1

p-values are computed as described by Nicholls [74], with lower values indicating more significance

the average EF(1 %) enrichment for Glide SP on the Glide exploratory set changes from 27.0 without water molecules to 26.9 with water molecules in the preparation. Similar small changes are observed for Glide HTVS. These results suggest that retaining water molecules for the preparation process and then eliminating them before docking is inconsequential, on average, to the overall enrichment results. However, this is an incomplete study on the role of waters in virtual screening and more work is needed to determine the best way to treat water molecules during docking. For example, it is possible to retain water molecules during docking, which was not explored here. In addition, the presence or absence of waters can be treated as additional degrees of freedom in the docking calculations, which has been tried by others [75–77]. To treat water molecules in a more meaningful way, it will be necessary not only to treat their presence or absence as additional degrees of freedom in the docking calculations, but also to consider the energetic consequences of displacing, bridging, trapping, or avoiding binding site waters. Recent progress in the field has brought us closer to understanding the thermodynamic characteristics of binding site waters [78, 79] and successful attempts have been made to produce a composite scoring function that accounts for the energetics of explicit waters [80, 81]. Future work will incorporate this information into the virtual screening process.

Variations in PDB structures

Finally, we explored the variation in enrichment observed for different crystal structures of the same target. The average range of EF(1 %) between targets with multiple crystals in the exploratory set is 11.9 (see Table 1), highlighting the known sensitivity of enrichment results to the choice of crystal structure. Similar variations have been shown in recent ensemble docking studies [46, 47, 82]. The greatest variation comes from COX2, in which 1cvu with Full + Ligand preparation produces an EF(1 %) of only 6.1 whereas 1cx2 results in an EF(1 %) of 33.7. However, upon closer investigation it was found that 1cvu is not a wild-type sequence of COX-2, as it contains an important

active site mutation of His207 to Ala. Therefore, the poor screening results with 1cvu might be expected, since active ligands might not bind as well (or at all) with His207 mutated to Ala.

Notable EF(1 %) enrichment changes in the other targets include estrogen receptor (range of 20.3), neuraminidase (range of 15.1), and thrombin (range of 12.7). Developing a method to choose a good single crystal structure for virtual screening is beyond the scope of this work. However, the variations seen here clearly demonstrate the importance of receptor structure selection and the need for a method to facilitate the receptor structure selection process.

Conclusions

In this work, we have presented a thorough study of the steps involved in protein and ligand preparation and the implications for structure-based virtual screening enrichments. We found that more complete preparation does indeed produce better virtual screening enrichments. The best virtual screening enrichments were obtained with a full preparation of the protein and inclusion of energetically accessible ligand ionization/tautomeric states. While the results were in line with expectations, a number of interesting findings arose from this study. First, performing an intermediate level of preparation, which includes predicting the hydrogen bonding network, but not minimizing the protein geometry, provided only a small improvement in enrichment results over minimizing only hydrogen coordinates. The full protein preparation, which includes both H-bond network optimization and geometry minimization, was needed to obtain significantly better results than the minimal preparation. In addition, a further gain in enrichment was observed when the energetic penalty for the ligand states, as computed by Epik, was added to the GlideScore. A number of examples were presented to illustrate the various changes that accounted for the differences in enrichments. Of notable interest were cases where proper protein preparation did not result in better scoring of actives, but resulted in worse scoring of decoys due to the elimination of unphysical protein or ligand states.

While many parameters were explored in this work, it was not an exhaustive study. For example, we only explored water molecules to the extent that they should be retained or removed before the preparation process. A more complete treatment would include the ability for waters to be explicitly included in the docking calculations so that they could be displaced, bridged, trapped, or avoided. In addition, the energetics of the water molecules in the aforementioned scenarios should be considered. In addition, we made no efforts to model residues with missing density or multiple occupancy. While there were not many residues around the binding sites with missing atoms or multiple occupancy, it is possible that changes in the results could be observed with differing treatments of atoms with missing density. Studying the effects of different crystal structure refinement protocols and how to deal with missing density and multiple occupancy will be the focus of a future study from our group where we explore the inclusion of x-ray diffraction data in the refinement protocols. Another limitation in this study was the docking to only a single rigid receptor structure. Recent results using Glide suggest that significantly better results can be obtained by using a well-selected structural ensemble [25]. We plan to pursue these points in more detail in future work.

References

1. Pierce AC, Jacobs M, Stuver-Moody C (2008) J Med Chem 51(6):1972
2. Hao W, Hu Y, Niu C, Huang X, Chang CPB, Gibbons J, Xu J (2008) Bioorg Med Chem Lett 18(18):4988
3. Salam NK, Huang TH-W, Kota BP, Kim MS, Li Y, Hibbs DE (2008) Chem Biol Drug Des 71(1):57
4. Kenyon V, Chorny I, Carvajal WJ, Holman TR, Jacobson MP (2006) J Med Chem 49(4):1356
5. Li H, Huang J, Chen L, Liu X, Chen T, Zhu J, Lu W, Shen X, Li J, Hilgenfeld R (2009) J Med Chem 52(15):4936
6. Shah F, Gut J, Legac J, Shivakumar D, Sherman W, Rosenthal PJ, Avery MA (2012) J Chem Inf Model 52(3):696
7. Kitchen DB, Decornez H, Furr JR, Bajorath J (2004) Nat Rev Drug Disc 3(11):935
8. Perola E, Walters WP, Charifson PS (2004) Proteins Struct Funct Bioinf 56(2):235
9. Kellenberger E, Rodrigo J, Muller P, Rognan D (2004) Proteins Struct Funct Bioinf 57(2):225
10. Sutherland JJ, Nandigam RK, Erickson JA, Vieth M (2007) J Chem Inf Model 47(6):2293
11. McGaughey GB, Sheridan RP, Bayly CI, Culberson JC, Kreatsoulas C, Lindsley S, Maiorov V, Truchon J-F, Cornell WD (2007) J Chem Inf Model 47(4):1504
12. Warren GL, Andrews CW, Capelli AM, Clarke B, LaLonde J, Lambert MH, Lindvall M, Nevins N, Semus SF, Senger S (2006) J Med Chem 49(20):5912
13. Cross JB, Thompson DC, Rai BK, Baber JC, Fan KY, Hu Y, Humblet C (2009) J Chem Inf Model 49(6):1455
14. Stahl M, Rarey M (2001) J Med Chem 44(7):1035
15. Schulz-Gasch T, Stahl M (2003) J Mol Model 9(1):47
16. Bissantz C, Folkers G, Rognan D (2000) J Med Chem 43(25):4759
17. Cummings MD, DesJarlais RL, Gibbs AC, Mohan V, Jaeger EP (2005) J Med Chem 48(4):962
18. Chen YZ, Zhi DG (2001) Proteins Struct Funct Bioinf 43(2):217
19. Santiago DN, Pevzner Y, Durand AA, Tran M, Scheerer RR, Daniel K, Sung S-S, Lee Woodcock H, Guida WC, Brooks WH (2012) J Chem Inf Model 52(8):2192
20. Huggins DJ, Sherman W, Tidor B (2012) J Med Chem 55(4):1424

21. Paul N, Kellenberger E, Bret G, Müller P, Rognan D (2004) Proteins Struct Funct Bioinf 54(4):671
22. Feher M, Williams CI (2012) J Chem Inf Model 52(3):724
23. Corbeil CR, Moitessier N (2009) J Chem Inf Model 49(4):997
24. Santos R, Hritz J, Oostenbrink C (2009) J Chem Inf Model 50(1):146
25. Repasky MP, Murphy RB, Banks JL, Greenwood JR, Tubert-Brohman I, Bhat S, Friesner RA (2012) J Comput Aided Mol Des 26(6):787
26. Goodsell DS, Olson AJ (1990) Proteins Struct Funct Bioinf 8(3):195
27. Kuntz ID, Blaney JM, Oatley SJ, Langridge R, Ferrin TE (1982) J Mol Biol 161(2):269
28. Jones G, Willett P, Glen RC, Leach AR, Taylor R (1997) J Mol Biol 267(3):727
29. Friesner RA, Banks JL, Murphy RB, Halgren TA, Klicic JJ, Mainz DT, Repasky MP, Knoll EH, Shelley M, Perry JK, Shaw DE, Francis P, Shenkin PS (2004) J Med Chem 47(7):1739
30. Verdonk ML, Cole JC, Hartshorn MJ, Murray CW, Taylor RD (2003) Proteins Struct Funct Genet 52(4):609
31. Halgren TA, Murphy RB, Friesner RA, Beard HS, Frye LL, Pollard WT, Banks JL (2004) J Med Chem 47(7):1750
32. Jain AN (2007) J Comput Aided Mol Des 21(5):281
33. Verdonk ML, Berdini V, Hartshorn MJ, Mooij WTM, Murray CW, Taylor RD, Watson P (2004) J Chem Inf Comput Sci 44(3):793
34. Friesner RA, Murphy RB, Repasky MP, Frye LL, Greenwood JR, Halgren TA, Sanschagrin PC, Mainz DT (2006) J Med Chem 49(21):6177
35. Graves AP, Shivakumar DM, Boyce SE, Jacobson MP, Case DA, Shoichet BK (2008) J Mol Biol 377(3):914
36. Morris GM, Goodsell DS, Halliday RS, Huey R, Hart WE, Belew RK, Olson AJ (1998) J Comput Chem 19(14):1639
37. Stroganov OV, Novikov FN, Stroylov VS, Kulkov V, Chilov GG (2008) J Chem Inf Model 48(12):2371
38. Claussen H, Buning C, Rarey M, Lengauer T (2001) J Mol Biol 308(2):377
39. Sherman W, Day T, Jacobson MP, Friesner RA, Farid R (2006) J Med Chem 49(2):534
40. Nabuurs SB, Wagener M, de Vlieg J (2007) J Med Chem 50(26):6507
41. Moitessier N, Therrien E, Hanessian S (2006) J Med Chem 49(20):5885
42. Corbeil CR, Englebienne P, Moitessier N (2007) J Chem Inf Model 47(2):435
43. Liu M, Bender SA, Cuny GD, Sherman W, Glicksman M, Ray SS (2013) Biochemistry (Mosc) 52(10):1725
44. Beuming T, Sherman W (2012) J Chem Inf Model 52(12):3263
45. Sherman W, Beard HS, Farid R (2006) Chem Biol Drug Des 67(1):83
46. Osguthorpe DJ, Sherman W, Hagler AT (2012) J Phys Chem B 116(23):6952
47. Osguthorpe DJ, Sherman W, Hagler AT (2012) Chem Biol Drug Design 80(2):182
48. Cavasotto CN, Abagyan RA (2004) J Mol Biol 337(1):209
49. Ferrari AM, Wei BQ, Costantino L, Shoichet BK (2004) J Med Chem 47(21):5076
50. Broughton HB (2000) J Mol Graph Modell 18(3):247
51. Rao S, Sanschagrin PC, Greenwood JR, Repasky MP, Sherman W, Farid R (2008) J Comput Aided Mol Des 22(9):621
52. Salam NK, Nuti R, Sherman W (2009) J Chem Inf Model 49(10):2356
53. 1 K Drug-Like Ligand Decoys Set. http://www.schrodinger.com/productpage/14/5/79/. Accessed 2012. Schrodinger, Inc.
54. Huang N, Shoichet BK, Irwin JJ (2006) J Med Chem 49(23):6789
55. LigPrep v2.5. Portland, OR: Schrödinger, Inc.; 2011
56. Epik v2.2. Portland, OR: Schrödinger, Inc.; 2011
57. Shelley JC, Cholleti A, Frye LL, Greenwood JR, Timlin MR, Uchimaya M (2007) J Comput Aided Mol Des 21(12):681
58. Bernstein FC, Koetzle TF, Williams GJB, Meyer EF, Brice MD, Rodgers JR, Kennard O, Shimanouchi T, Tasumi M (1977) J Mol Biol 112(3):535
59. Berman HM, Westbrook J, Feng Z, Gilliland G, Bhat TN, Weissig H, Shindyalov IN, Bourne PE (2000) Nucleic Acids Res 28(1):235
60. Maestro v9.2. Portland, OR: Schrödinger, Inc.; 2011
61. Banks JL, Beard HS, Cao Y, Cho AE, Damm W, Farid R, Felts AK, Halgren TA, Mainz DT, Maple JR, Murphy R, Philipp DM, Repasky MP, Zhang LY, Berne BJ, Friesner RA, Gallicchio E, Levy RM (2005) J Comput Chem 26:1752
62. Jorgensen WL, Tirado-Rives J (1988) J Am Chem Soc 110:1657
63. Kaminski GA, Friesner RA, Tirado-Rives J, Jorgensen WL (2001) J Phys Chem B 105(28):6474
64. Shivakumar D, Williams J, Wu Y, Damm W, Shelley J, Sherman W (2010) J Chem Theory Comput 6(5):1509
65. Österberg F, Morris GM, Sanner MF, Olson AJ, Goodsell DS (2002) Proteins Struct Funct Genet 46(1):34
66. Rarey M, Kramer B, Lengauer T (1999) Proteins Struct Funct Bioinf 34(1):17
67. Verdonk ML, Chessari G, Cole JC, Hartshorn MJ, Murray CW, Nissink JWM, Taylor RD, Taylor R (2005) J Med Chem 48(20):6504
68. de Graaf C, Oostenbrink C, Keizers PHJ, van der Wijst T, Jongejan A, Vermeulen NPE (2006) J Med Chem 49(8):2417
69. Myrianthopoulos V, Kritsanida M, Gaboriaud-Kolar N, Magiatis P, Ferandin Y, Durieu E, Lozach O, Cappel D, Soundararajan M, Filippakopoulos P, Sherman W, Knapp S, Meijer L, Mikros E, Skaltsounis A-L (2012) ACS Medicinal Chem Lett 4(1):22
70. Beuming T, Che Y, Abel R, Kim B, Shanmugasundaram V, Sherman W (2011) Proteins Struct Funct Bioinf 80:871
71. Glide v5.7. Portland, OR: Schrödinger, Inc.; 2011
72. Truchon J-F, Bayly CI (2007) J Chem Inf Model 47(2):488
73. Bird LE, Ren J, Wright A, Leslie KD, Degreve B, Balzarini J, Stammers DK (2003) J Biol Chem 278(27):24680
74. Nicholls A (2008) J Comput Aided Mol Des 22(3):239
75. de Beer S, Vermeulen NPE, Oostenbrink C (2010) Curr Top Med Chem 10(1):55
76. Katritch V, Jaakola V-P, Lane JR, Lin J, Ijzerman AP, Yeager M, Kufareva I, Stevens RC, Abagyan R (2010) J Med Chem 53(4):1799
77. Huang N, Shoichet BK (2008) J Med Chem 51(16):4862
78. Abel R, Young T, Farid R, Berne BJ, Friesner RA (2008) J Am Chem Soc 130(9):2817
79. Young T, Abel R, Kim B, Berne BJ, Friesner RA (2007) PNAS 104:808
80. Abel R, Salam NK, Shelley J, Farid R, Friesner RA, Sherman W (2011) ChemMedChem 6(6):1049
81. Guimaraes CRW, Mathiowetz AM (2010) J Chem Inf Model 50(4):547
82. Kalid O, Warshaviak DT, Shechter S, Sherman W, Shacham S (2012) J Comput Aided Mol Des 26(11):1217